31st Congress of the International Council of the Aeronautical Sciences
Belo Horizonte, Brazil; September 09-14, 2018

NUMERICAL STUDY OF REYNOLDS NUMBER EFFECT ON SUPERCRITICAL WING AERODYNAMIC LOADS

Qian Guangping1*, SI Jiangtao, LIU Kaili****
***Shanghai Aircraft Design and Research Institute**

Keywords: *Reynolds number ; Aerodynamic loads ; Supercritical Wing ; Pressure center*

Abstract

Numerical simulations are performed to investigate the effect of Reynolds number on supercritical wing aerodynamic loads. Solutions at both wind tunnel Reynolds number and flight Reynolds number are numerical computed. The Reynolds number effect on wing chord wise aerodynamic loads, span wise aerodynamic loads and components loads allot is investigated. The numerical results indicate that the supercritical wing chord wise loads, pressure center move aft and torsion loads increase when Reynolds number increases from 4000000 to 24000000 in cruise. The supercritical wing span wise pressure center moves outside with the increase of Reynolds numbers in cruise. The nose down moment increases resulting in the increase of trim loads of horizontal tail. it will lead to structure design risk without the Reynolds number correction of wing loads distribution.

1 General Introduction

The load is the initial data which evaluates aircraft's structure integrality in the whole lifecycle(including structural strength, stiffness, durability, damage tolerance analysis and test). So it is vital for the aircraft's security and the decrease of the structural weight to confirm the load properly. The technology of load confirmation is one of the ten key technologies that our country must capture for the development of large civil aircraft according to some domestic authoritative experts. Security and economy and comfort are the main consideration of civil aircraft comparing with military aeroplane. It can reduce structural weight, meet the reliability and security, improve economy.

Recently, the aerodynamic data which is the base of the flight load calculation for domestic civil aircraft is from wind tunnel test. The Reynolds number of wind tunnel test of high speed and low speed for civil aircraft is greatly less than flight Reynolds number because of the limitation of test condition. Usually, the Reynolds number of the whole model high speed force test and half model low speed pressure test for single aisle airplane is 4 million while the corresponding flight Reynolds number is 24 million. It adopts supercritical airfoil which are characterized by their flatted upper surface(suction side surface),highly cambered aft section, and greater leading edge radius compared with conventional airfoil shapes for modern civil airplane. Flows about supercritical airfoil are shown to be particularly sensitive to viscosity and Reynolds number. The Reynolds number affects directly the shock wave location, strength, the interference between shock wave and boundary layer, separation. It affects subsequently aerodynamic load, the position of pressure center, aerodynamic derivative and coefficient which affects the load distribution between wing and empennage.

For the design of American C-141aircraft, it nearly results in plane crash that the key influence is the low wind tunnel Reynolds due to the insufficiency of Reynolds number effect study. The chord-wise pressure distribution differ greatly between flight test and wind tunnel test shown in Fig.1. The position of shock wave in flight moves aft about 20% of chord comparing with wind tunnel test, the variation of pitch moment about 11% which leads to the redesign of the wing and the weight increase about 180kg. Hence, it must validate the load through flight test if the wing pressure distribution is the base of the

load calculation in the design of new airplane according to the airworthiness authority.

To avoid the error of load calculation which results from wind tunnel test data, this paper presents some numerical study about the wing aerodynamics difference between wind tunnel Reynolds number and flight test Reynolds number acquiring exact chord-wise and spanwise aerodynamic load, pressure centre and aerodynamic derivative for flight load calculation.

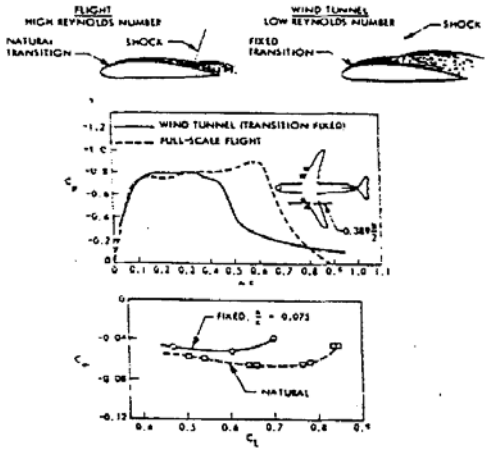

图 1C-141 飞机气动特性变化

2 Computational methodology

2.1 Governing equation

2.1.1 Full-potential equation

The unsteady full-potential equation written in a body fitted coordinate system is given by

$$(\rho J)_\tau + (\rho U J)_\xi + (\rho V J)_\eta + (\rho W J)_\zeta = 0 \qquad (1)$$

where ρ is density, U, V, and W are the contravariant velocity components in the ξ, η, and ζ, directions, τ means time, and J is Jacobian. Eq. (1) is solved by the time-accurate approximate factorization algorithm and internal Newton iterations; body conditions and wake conditions are implicit embedded.

2.1.2 Boundary layer equation

The original system of differential equations, which governs the gas flow in the three-dimensional boundary layer has the form:

$$\left.\begin{aligned}
&\frac{\partial}{\partial x}(\rho u h_2 \sin\theta) + \frac{\partial}{\partial z}(\rho w h_1 \sin\theta) + \frac{\partial}{\partial y}(\rho v h_1 h_2 \sin\theta) = 0 \\
&\rho\frac{u}{h_1}\frac{\partial u}{\partial x} + \rho\frac{w}{h_2}\frac{\partial u}{\partial z} + \overline{\rho v}\frac{\partial u}{\partial y} - \rho k_1 u^2 \cot\theta + \rho k_2 w^2 \csc\theta + \rho k_{12} uw = \\
&\qquad = -\frac{\csc^2\theta}{h_1}\frac{\partial p}{\partial x} + \frac{\csc\theta\cot\theta}{h_2}\frac{\partial p}{\partial z} + \frac{\partial}{\partial y}\left(\mu\frac{\partial u}{\partial y} - \overline{\rho u' v'}\right) \\
&\rho\frac{u}{h_1}\frac{\partial w}{\partial x} + \rho\frac{w}{h_2}\frac{\partial w}{\partial z} + \overline{\rho v}\frac{\partial w}{\partial y} - \rho k_2 w^2 \cot\theta + \rho k_1 u^2 \csc\theta + \rho k_{21} uw = \\
&\qquad = -\frac{\cot\theta\csc\theta}{h_1}\frac{\partial p}{\partial x} + \frac{\csc^2\theta}{h_2}\frac{\partial p}{\partial z} + \frac{\partial}{\partial y}\left(\mu\frac{\partial w}{\partial y} - \overline{\rho w' v'}\right)
\end{aligned}\right\} \qquad (2)$$

where $\overline{\rho v} = \rho v + \overline{\rho' v'}$.

The coordinate *y* is directed along the normal to the wing surface, the variables *x*, *z* govern the system of non-orthogonal coordinates with angle $\theta(x,z)$ between them on the surface, *u*,*v*,*w* - are the components of the velocity vector along the coordinates *x*,*y*,*z*, ρ- is the density, *p* - is the pressure, μ - is the dynamic viscosity coefficient, $h_1 = \partial s_1/\partial x$, $h_2 = \partial s_2/\partial x$ are the metric coefficients.

The parameters k_1, k_2, k_{12}, k_{21} characterize curvature of coordinate lines *z*=const, *x*=const. has form:

$$k_1 = \frac{1}{h_1 h_2 \sin\theta}\left[\frac{\partial}{\partial x}(h_2\cos\theta) - \frac{\partial h_1}{\partial z}\right]$$

$$k_2 = \frac{1}{h_1 h_2 \sin\theta}\left[\frac{\partial}{\partial z}(h_1\cos\theta) - \frac{\partial h_2}{\partial x}\right]$$

$$k_{12} = \frac{1}{\sin\theta}\left[-\left(k_1 + \frac{1}{h_1}\frac{\partial\theta}{\partial x}\right) + \cos\theta\left(k_2 + \frac{1}{h_2}\frac{\partial\theta}{\partial z}\right)\right]$$

$$k_{21}=\frac{1}{\sin\theta}\left[-\left(k_2+\frac{1}{h_2}\frac{\partial\theta}{\partial z}\right)+\cos\theta\left(k_1+\frac{1}{h_1}\frac{\partial\theta}{\partial x}\right)\right]$$

The boundary conditions are as follows:

on the external edge of the boundary layer:

$$y=\delta,\quad u=u_e(x,z),\quad w=w_e(x,z)$$

on the wall:

$$y=0,\quad u=w=0\quad v_w=0$$

2.2 Viscous-inviscid interaction

For the determination of self-consistent solutions the quasi-simultaneous coupling scheme is used. It allows one to take into account the expected boundary layer response to the chordwise velocity variation while calculating the external flow, and ensures effective and rapid computation of viscid-inviscid interaction including moderate separation regimes.

3 Computational validation

To validate the flowfield computation method, the DLR-F6 model was numerically simulated and compared with the experimental data at CL=0.57. The DLR-F6 model is a twin-engine aircraft model, with a variety of wind-tunnel experiment data and numerical solutions available over years. The nacelle of DLR-F6 is a through flow nacelle. Fig. 2 shows the variation of CL with the number of grid points for the DLR-F6 wing-body/nacelle, indicating that the 600000 grid points are adequate for this simulation. The computational grid for the DLR-F6 wing-body/nacelle (600000 grid points) is presented in Fig. 3.

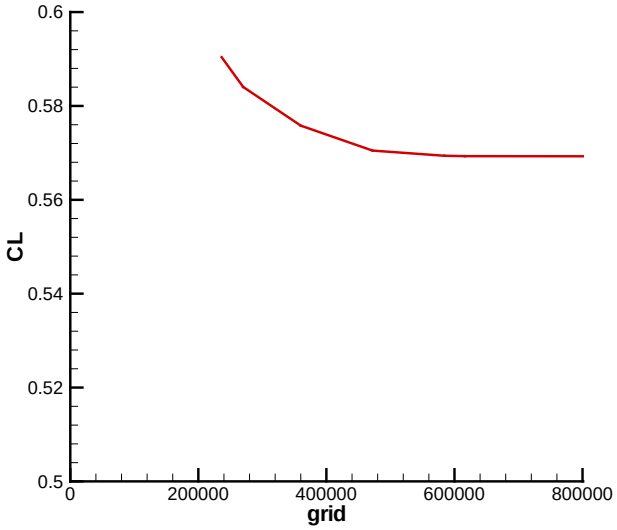

Fig. 2 The variation of CL with the number of grid points.

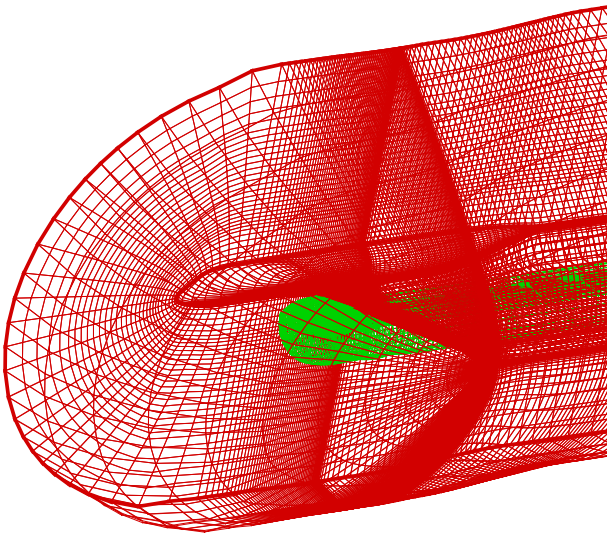

Fig. 3 DLR-F6 wing-body/nacelle grid.

The wing pressure distributions from the present computation and experiments are shown in Fig. 4, respectively, with Ma=0.75, CL= 0.4 and Reynolds number of 3×10^6 based on the mean aerodynamic chord. The lift-to-drag characteristics between the calculations and experiments are shown in Fig. 5.The simulated results are in excellent agreement with the experiments, showing that the grid generation strategy and numerical method are adequate for this case. Thus, overall, the simulation gives a satisfactory prediction of pressure distribution, lift-to-drag characteristics and is therefore considered to be a satisfactory basis for determining simulations.

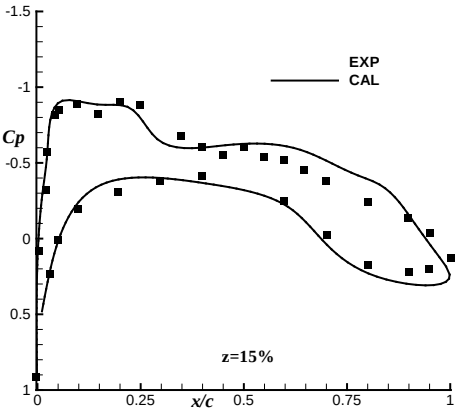

(a) at z=15%

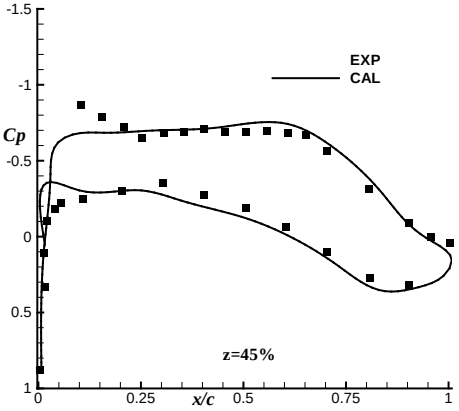

(b) at z=45%

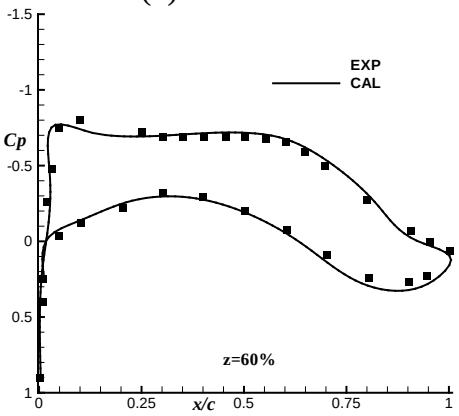

(c) at z=60%

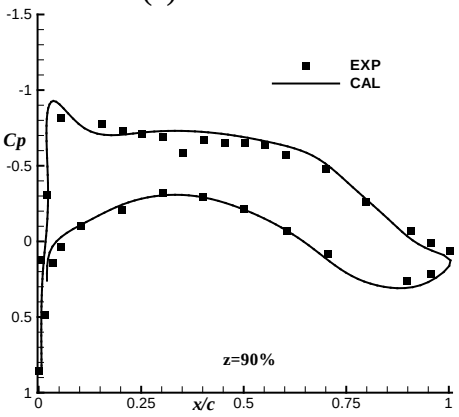

(d) at z=90%

Fig. 4 Wing surface Cp comparison at Ma=0.75.

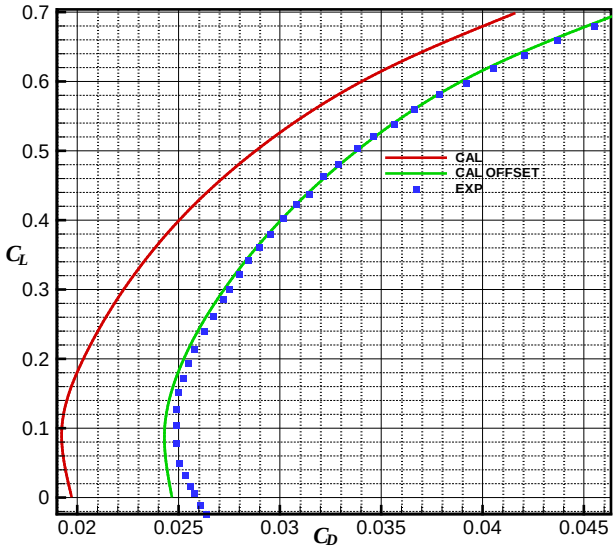

Fig. 5 Lift-to-drag characteristics comparison at Ma=0.75.

4 Results and discussion

Taking a supercritical wing aircraft for instance, a numerical simulation is performed. Comparison analysis is conducted at the mach number of 0.785,0.82 and the Reynolds number of 4 million, 24 million.

4.1 Reynolds number effects on chord-wise pressure distribution

The numerical results of Reynolds number effects on chord-wise pressure distribution for both upper surface and lower surface are presented in Figs. 6-9.

It proclaims that Reynolds number has obviously effects on pressure distribution of upper surface and lower surface.

In the upper surface which has separation induced by shock wave, the viscidity effect weakens as the increase of Reynolds number. The shock wave moves aft , the strength of shock wave increases, the pressure roof descends.

The increase of Reynolds number has greatly effects on aft loading of lower surface while the aft loading increases and the fore loading decreases. The influence on outer wing is more obvious thanks to the lower local Reynolds number and wingtip effect of sweepback wing, especially in the presence of shock wave.

The Reynolds number effect grows, shock wave moves aft greatly, the aft loading strengthens as the increase of mach number at the same lift coefficient.

The Reynolds number has greater effect on shock wave location as the increase of lift coefficient at the same mach number while the Reynolds number effect on aft loading weakens as the airstream velocity of lower surface decreases.

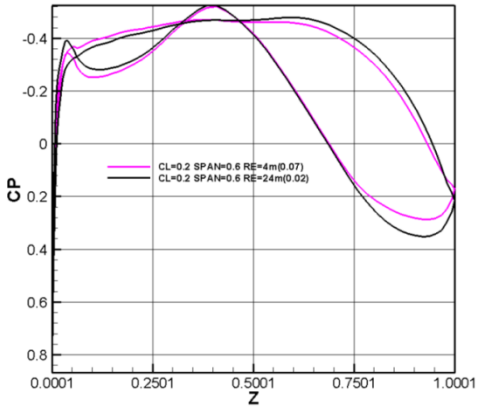

Fig. 6 The comparison of wing pressure distribution at Ma=0.785,CL=0.2.

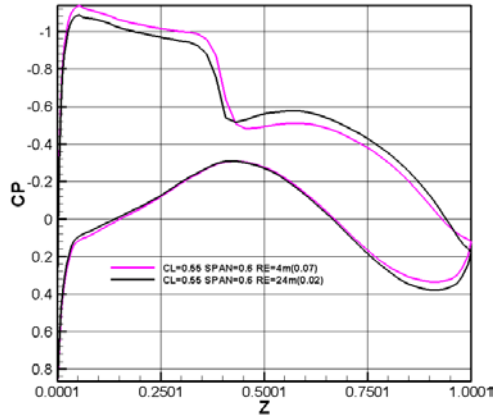

Fig. 7 The comparison of wing pressure distribution at Ma=0.785,CL=0.5.

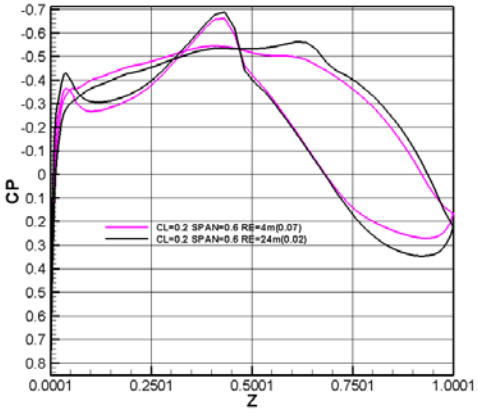

Fig. 8 The comparison of wing pressure distribution at Ma=0.82,CL=0.2.

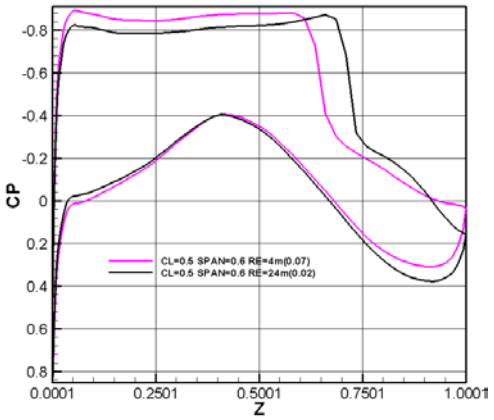

Fig. 9 The comparison of wing pressure distribution at Ma=0.82,CL=0.5.

4.2 Reynolds number effects on chord-wise pressure centre

The Reynolds number effect on wing chord-wise pressure distribution leads to the variation of chord-wise pressure centre consequentially according to Figs. 10-12.

The wing chord-wise pressure centre moves aft, as the increase of Reynolds number and mach number at the same lift coefficient. It has larger motion quantity backwards for the wingtip area because of the lower local Reynolds number.

The motion quantity backwards of chord-wise pressure centre decreases as the increase of lift coefficient at the same mach number because the influence on pressure centre due to aft loading is larger than the one due to shock wave.

The motion quantity backwards chord-wise pressure centre is about 4.5%-8.5%MAC at lower lift coefficient while the quantity is about 2%—5%MAC at lower lift coefficient. It is obvious for the variation chord-wise pressure centre.

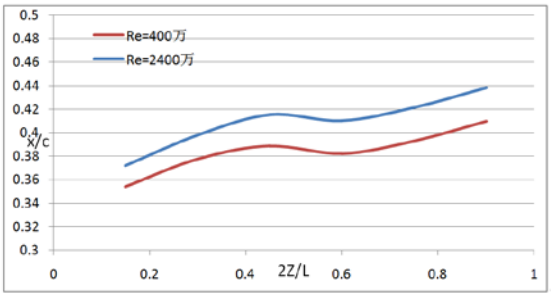

图8机翼弦向压心位置对比(Ma=0.785，CL=0.5)

Fig. 10 The comparison of chord-wise pressure centre at Ma=0.785,CL=0.5.

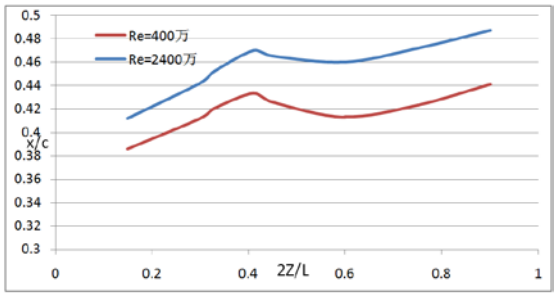

Fig. 11 The comparison of chord-wise pressure centre at Ma=0.782,CL=0.5.

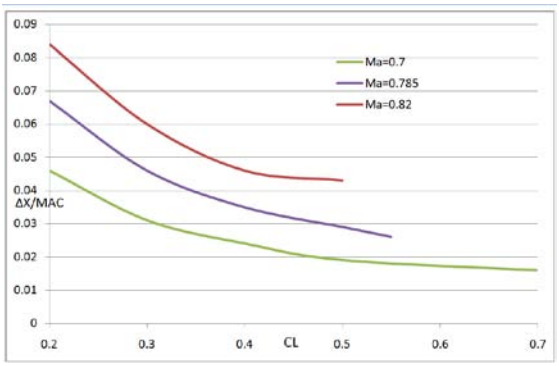

Fig. 12 The comparison of chord-wise pressure centre motion quantity backwards.

4.3 Reynolds number effects on span-wise aerodynamic load

The Reynolds number effect on wing chord-wise aerodynamic load results in the variation of chord-wise aerodynamic load consequentially according to Figs. 13-15.

The circulation at wing root decreases as the increase of Reynolds number at the same lift coefficient while the circulation at wing tip increases, consequently the span-wise pressure centre moves outwards because of the movement backwards of shock wave, the increase of aft loading and lift. The Reynolds number effect at the wing tip area is larger than the one at the root which will lead to the lift increase at the wing tip area and the lift decrease at the root.

The variation of span-wise load certainly leads to the variation of span-wise pressure centre as shown in Figs. 13-15.

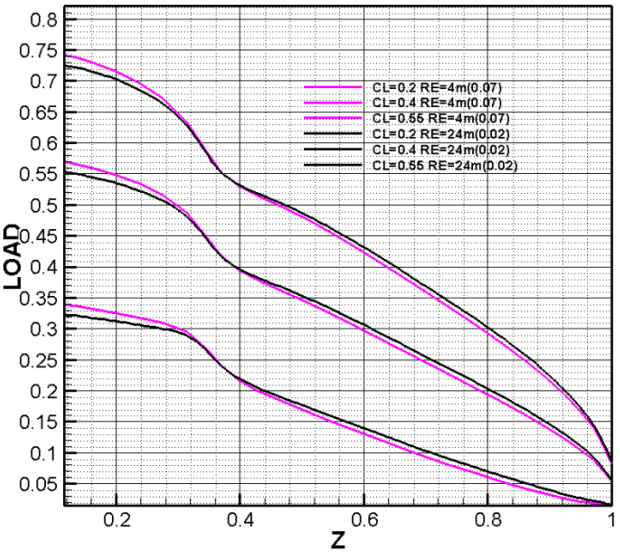

Fig. 13 The variation of wing span-wise circulation versus Reynolds number at Ma=0.785.

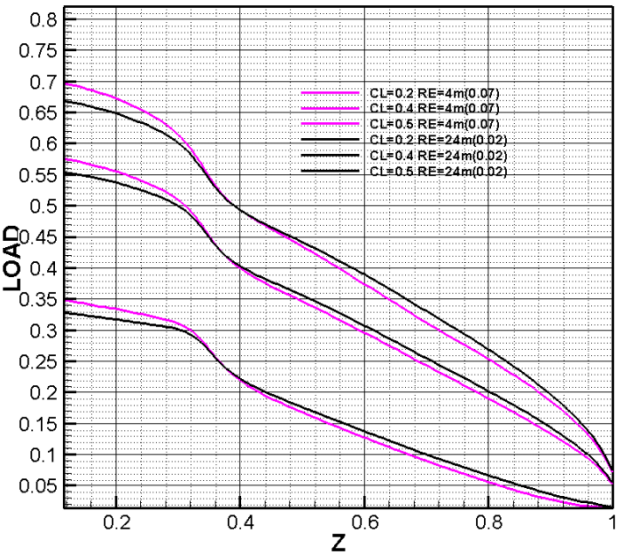

Fig. 14 The variation of wing span-wise circulation versus Reynolds number at Ma=0.82.

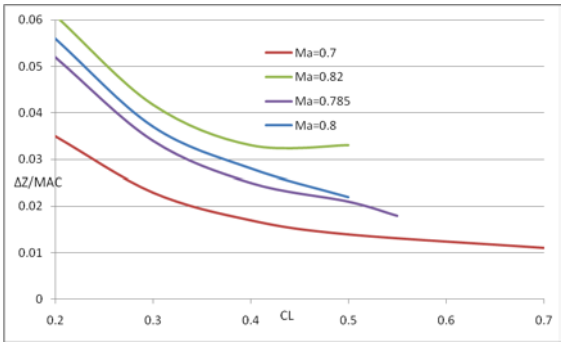

Fig. 15 The variation of wing span-wise pressure centre versus lift coefficient.

The Reynolds number effect is much more obvious, the variation of span-wise pressure centre is larger as the increase of mach number at the same lift coefficient. The variation of span-wise pressure centre is smaller as the decrease of lift coefficient at the mach number.
The variation of span-wise pressure centre is about 3.5%—6.0%MAC at lower lift coefficient while the one at higher lift coefficient is about 1%—3.5%MAC.

4.4 Reynolds number effects on aerodynamic load distribution among aircraft's components

The increase of Reynolds number has less effect on normal load of no-tail configuration aircraft, about 2% while it has obvious effect on horizontal tail load, about 84% at weight centre of 44%MAC n=1, about 83% at weight centre of 17%MAC n=2.5 according to Figs. 16-19. The main reason is the increase of pitch down moment of no-tail configuration aircraft as the increase of Reynolds number. So it is reasonable to calculate load through the aerodynamic data after Reynolds number correction to choose accurate severe load case.

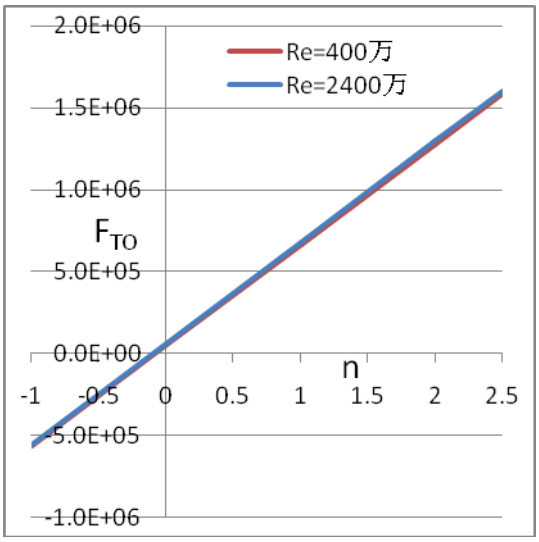

Fig. 16 The comparison of no-tail aerodynamic load in checked maneuver(Ma=0.82，H=7492m，weight centre of 44%MAC).

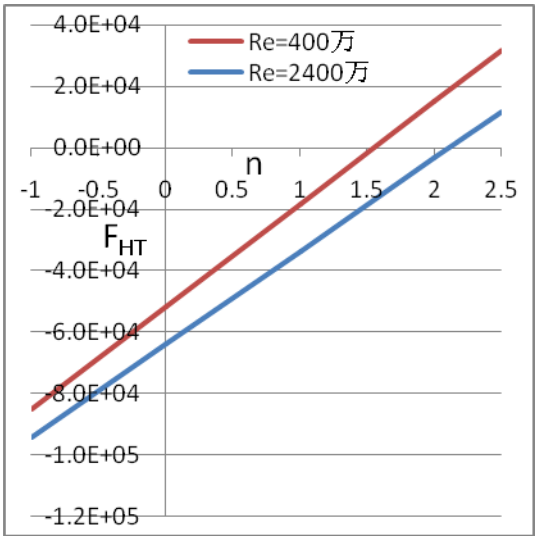

Fig. 17 The comparison of horizontal tail aerodynamic load in checked maneuver(Ma=0.82，H=7492m，weight centre of 44%MAC).

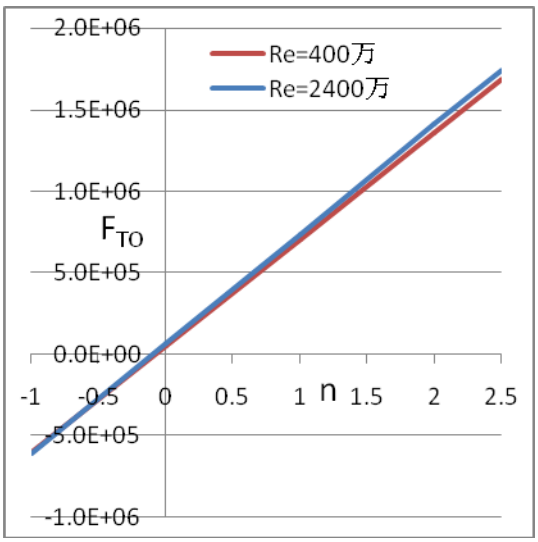

Fig. 18 The comparison of no-tail aerodynamic load in checked maneuver(Ma=0.82，H=7492m，weight centre of 17%MAC).

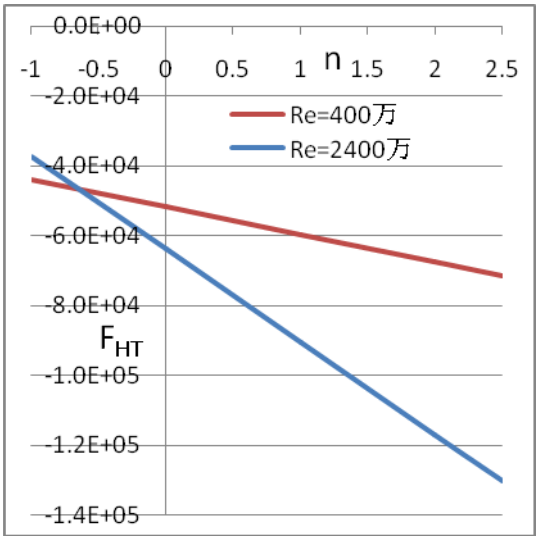

Fig. 19 The comparison of horizontal tail aerodynamic load in checked maneuver(Ma=0.82，H=7492m，weight centre of 17%MAC).

5 Conclusions

In this work, we presented the numerical simulation results of Reynolds number effects on aerodynamic load for supercritical wing aircraft acquiring its effect on aerodynamic load and the distribution among aircraft's components. The following conclusions are drawn.

1) The chord-wise pressure centre moves aft, the span-wise pressure centre moves outwards, the load of bend, twist and shear increase when the Reynolds increases from 4 million to 24 million in cruise. So it has much more influence on the wing's flutter. The load on horizontal tail increases while the pitch down moment increases, especially in higher overload.

2) Usually, it only corrects the total load, not correct component load according to Reynolds number effect through the data from wind tunnel test. This work can correct both total load and component load supplying more accurate load to reduce the design cost before high Reynolds number wind tunnel test.

3) The results from this work has an important significance in flight load calculation, especially for long range wide-body aircraft with higher Reynolds number.

6 Contact Author Email Address

My email address: qianguangping@comac.cc

Copyright Statement